JCTC Journal of Chemical Theory and Computation

Active-Space Equation-of-Motion Coupled-Cluster Methods through Quadruples for Excited, Ionized, and Electron-Attached States

Peng-Dong Fan, Muneaki Kamiya, and So Hirata*

Quantum Theory Project, Department of Chemistry, University of Florida, Gainesville, Florida 32611-8435

Received August 17, 2006

Abstract: Several variants of the equation-of-motion coupled-cluster (EOM-CC) method with singles (one-hole or one-particle), doubles (two-hole-one-particle or two-particle-one-hole), and a selected set of triples (three-hole-two-particle or three-particle-two-hole) and/or quadruples (four-hole-three-particle or four-particle-three-hole) have been implemented by computerized symbolic algebra. They are applicable to excitation energies (EE), ionization potentials (IP), and electron affinities (EA), excited-state dipole moments, and transition dipole moments of both closed- and open-shell species and are abbreviated as EE/IP/EA-EOM-CCSD*t*, EE/IP/EA-EOM-CCSD*tq*, and EE/IP/EA-EOM-CCSDT*q*, where the small letters indicate the use of active-space cluster and EE/IP/EA operators. They are also parallel executable and accelerated by the use of spin, spatial, and permutation symmetries. The remarkable effectiveness of the methods in capturing nondynamical correlation effects has been demonstrated by their applications to the vertical excitation energies of C_2, the adiabatic excitation energies and dipole moments of the CH radical, the adiabatic excitation energies of the CH_2 diradical, the adiabatic excitation energies and dipole moments of formaldehyde, the vertical ionization energies of N_2, and the vertical electron affinities of C_2. The effectiveness is found to decline when the basis set is extended, causing the active space to become relatively small and also less well-defined. As a remedy, we propose a composite method that combines higher-rank active-space methods with smaller basis sets for nondynamical correlation and lower-rank nonactive-space methods with larger basis sets for dynamical correlation, which is shown to work well for an excited-state potential energy curve of hydrogen fluoride.

I. Introduction

The most accurate and compact single-reference coupled-cluster (CC) descriptions[1−4] of electronic transitions can be furnished by the equation-of-motion (EOM) CC method[5−10] and the related CC linear response (LR)[11−17] and symmetry-adapted-cluster configuration-interaction (SAC-CI) methods.[18,19] They can handle not only excitation energies (EE)[7−10,20−25] but also ionization potentials (IP)[26−31] and electron affinities (EA).[32−35] The lowest-order member of the EOM-CC hierarchy for excitation energies (EE-EOM-CC), i.e., the EE-EOM-CC with singles and doubles (EE-EOM-CCSD),[7−10,25] has been established as a reliable method for dominantly single excitations. Its performance deteriorates when the excited states have significant double excitation components from the ground state, when the ground state itself is quasidegenerate, or when the entire excited-state potential energy surfaces are considered. Similarly, EOM-CCSD for ionization energies and electron affinities, i.e., IP-[26−29] and EA-EOM-CCSD,[32,33] prove inadequate for shake-up or shake-on transitions and when the effect of orbital relaxation is substantial. In these cases, higher-order EE/IP/EA-EOM-CC methods, such as those through triples

* Corresponding author e-mail: hirata@qtp.ufl.edu.

10.1021/ct600270c CCC: $37.00
Published on Web 03/20/2007

(EE-,[20,23] IP-,[30,31,36] and EA-EOM-CCSDT[34,35]) and through quadruples (EE-,[37,38] IP-,[31] and EA-EOM-CCSDTQ,[35]) become necessary. However, the high-rank polynomial size dependence of the computational cost of these methods, e.g., $O(n^8)$ of EE-EOM-CCSDT and $O(n^{10})$ of EE-EOM-CCSDTQ (n is the number of orbitals), prohibits their applications to large molecules, despite their correct theoretical size dependence (size extensivity and intensivity). The high-order EE/IP/EA-EOM-CC calculations are by no means routine, although the electronic states that demand these treatments are not uncommon.

The essential effects of higher-order excitation operators can nevertheless be incorporated in the coupled-cluster (CC) method at a low cost by the ansatz of Adamowicz and co-workers,[39−41] defining the active-space CC methods. It restricts higher-order cluster T operators to those that involve user-defined active orbitals, in ways that do not impair size extensivity. When nondynamical correlation effects calling for the high-order CC methods are plainly associated with a small set of orbitals, the active-space methods designating these orbitals as active can provide the most compact descriptions of these effects. The active-space CC methods through triples (CCSD*t*) and quadruples (CCSD*tq* and CCSDT*q*) (the small letters in acronyms indicate restricted triples and/or quadruples) have been implemented into parallel execution programs by us[42] with the aid of computerized symbolic algebra. Kállay and co-workers implemented a general-order CC method[43] with their string-based algorithm and subsequently incorporated the active-space ansatz into this.[44]

It is not unreasonable to expect that this class of methods is even more effective for excited, ionized, and electron-attached states because the proportion of double excitation, shake-up ionization, shake-on electron-attachment, and higher-ranked contributions in the wave functions can be much greater (and can reach unity) than the double excitation contributions in ground-state wave functions. The active-space ansatz was hence extended to excited states by Kowalski and Piecuch,[22,23] who reported the formalisms of EE-EOM-CCSD with active-space triples (EE-EOM-CCSD*t*) and quadruples (EE-EOM-CCSD*tq*) and an implementation of EE-EOM-CCSD*t*, where, in addition to T, higher-order excitation R (or deexcitation L) operators were restricted. Kowalski et al.[45] also reported a semiautomated parallel implementation of EE-EOM-CCSD*t*. Slipchenko and Krylov[46] implemented the spin-flip EOM-CCSD(2,3) method in addition to the usual spin-conserving counterpart, where only R and L included active-space triples, while T reached up to doubles. Gour et al.[47−49] applied the scheme to ionization energies and electron affinities, in which ionization $R^{(N-1)}$ and electron-attachment $R^{(N+1)}$ operators were restricted, implementing IP-EOM-CCSD*t* and EA-EOM-CCSD*t*. Kállay and Gauss[38] reported a general-order EE-EOM-CC for energies and properties employing the string-based algorithm that was fitted with the ability to apply active-space restrictions on any of the high-order cluster and linear excitation operators. Köhn and Olsen[50] generalized the active space by further dividing it into many subspaces and combined them with a general-order CC method in an algorithm similar to the string-based algorithm of Kállay and Surján.[43]

For a fixed active space size, the size dependence of computational cost remains $O(n^6)$ for EE-EOM-CCSD*t* and EE-EOM-CCSD*tq* and $O(n^5)$ for IP/EA-EOM-CCSD*t* and IP/EA-EOM-CCSD*tq*. In addition to this remarkable speedup, the active-space EOM-CC approach has several unmatched advantages: it substantiates the state-selective multireference CC method in a transparent and unambiguous single-reference framework; it reduces to the full EOM-CC methods when all orbitals are active; it can rival the full EE/IP/EA-EOM-CC methods in the ability to include essential high-order correlation and EE/IP/EA effects with a small active space; and it is size extensive for total energies and size intensive for transition energies.

In this article, we report implementations of a number of extensions to this method which have been made with the essential aid of the symbolic algebra system (Tensor Contraction Engine or TCE)[37,51−54] completely automating the time-consuming and error-prone processes of formula derivations and computer implementations involved. The original contributions of the present study are the following. We present the algebraic, order-by-order (as opposed to the so-called determinant-[55−58] or string-based[38,43]) implementations of the EE/IP/EA-EOM-CCSD*t*, EE/IP/EA-EOM-CCSD*tq*, and EE/IP/EA-EOM-CCSDT*q* methods and their numerous variants differing from each other in detailed definitions of active-space cluster and EE/IP/EA operators. Being based on spin-orbital formalisms, these TCE-synthesized programs can compute the excitation, ionization, and electron-attachment energies of closed- and open-shell molecules. Their execution is accelerated by distributed- or replicated-data load-balancing parallelism and the use of various symmetries (spin symmetry, real Abelian point-group symmetry, and index permutations). We also furnish the active-space EE-EOM-CC programs with the capability to compute transition dipole moments (and oscillator strengths) and excited-state dipole moments. This capability requires the left-hand-side eigenvectors of the non-Hermitian CC effective Hamiltonian in addition to the right-hand-side eigenvectors that are sufficient for excitation energies alone. The left-hand-side eigenvector corresponding to the ground state is related to the so-called Λ vector of the CC analytical gradient theory.[59] The Λ vectors and the ground-state dipole moments with the active-space CC (CCSD*t*, CCSD*tq*, and CCSDT*q*) methods have also become available by the present developments.

We also document the results of benchmark calculations of these active-space EOM-CC methods for the vertical excitation energies of C_2, the adiabatic excitation energies and dipole moments of the low-lying excited states of the CH radical, the adiabatic excitation energies and dipole moments of the low-lying excited states of formaldehyde, the adiabatic excitation energies of the CH_2 diradical, the vertical ionization energies of N_2, and the electron affinities of C_2. They attest to the remarkable accuracy of the active-space methods with the minimum active spaces: e.g., the errors from the full configuration-interaction (FCI) results in the vertical excitation energy to the $^1\Delta_g$ state of C_2

diminish rapidly from 2.1 eV (EOM-CCSD) to 0.24 eV (EOM-CCSD*t*) and to −0.06 eV (EOM-CCSD*tq*) as we introduce the active-space triples and quadruples. These applications also expose the methods' weaknesses. The effectiveness of the active-space triples and quadruples is increasingly less when the higher-than-double excitation effects are characterized as dynamical correlation and as the basis set is extended and the active space becomes relatively smaller and less well-defined. In lieu of the usual remedy of (variationally) optimizing the active orbitals,[60−62] we propose a composite method that combines higher-rank active-space methods with smaller basis sets for nondynamical correlation and lower-rank nonactive-space methods with larger basis sets for dynamical correlation, which is shown to work well for an excited-state potential energy curve of hydrogen fluoride.

II. Theory

In the EE-EOM-CC theory, the *k*th excited state of an atom or a molecule is defined as

$$|\Psi_k\rangle = R(k)|\Psi_0\rangle \tag{1}$$

where

$$|\Psi_0\rangle = \exp(T)|\Phi\rangle \tag{2}$$

is the ground-state CC wave function and $R(k)$ is a linear excitation operator. The k dependence of $R(k)$ will be dropped hereafter whenever it is not essential. $|\Phi\rangle$ is a single-reference wave function—usually, a Hartree−Fock (HF) determinant—and T is the cluster operator. The R and T operators are defined as

$$R = \sum_{n=0}^{m} R_n \tag{3a}$$

$$R_n = \left(\frac{1}{n!}\right)^2 r_{a_1\cdots a_n}^{i_1\cdots i_n} C^{a_1}\cdots C^{a_n} C_{i_n}\cdots C_{i_1} \tag{3b}$$

and

$$T = \sum_{n=1}^{m} T_n \tag{4a}$$

$$T_n = \left(\frac{1}{n!}\right)^2 t_{a_1\cdots a_n}^{i_1\cdots i_n} C^{a_1}\cdots C^{a_n} C_{i_n}\cdots C_{i_1} \tag{4b}$$

respectively, where $r_{a_1\cdots a_n}^{i_1\cdots i_n}$ and $t_{a_1\cdots a_n}^{i_1\cdots i_n}$ are amplitudes, and C^{a_n} (C_{i_n}) are the creation (annihilation) operators and m determines the rank of the EE-EOM-CC method. Indices i_1, ..., i_n and a_1, ..., a_n designate the occupied spin-orbitals in the reference $|\Phi\rangle$ and unoccupied spin-orbitals, respectively. We use, whenever possible, the Einstein summation convention over the repeated upper and lower indices.

The amplitudes $t_{a_1\cdots a_n}^{i_1\cdots i_n}$ of the T operator can be obtained by solving the CC equations

$$\langle\Omega|\bar{H}_N|\Phi\rangle = 0 \tag{5}$$

where $|\Omega\rangle$ is a manifold of single through m-tuple excitation determinants and $\bar{H}_N$ is a similarity-transformed Hamiltonian defined as

$$\bar{H}_N = \exp(-T)H_N\exp(T) = [H_N\exp(T)]_C \tag{6a}$$

$$H_N = H - \langle\Phi|H|\Phi\rangle \tag{6b}$$

where H is the usual electronic Hamiltonian. $[H_N\exp(T)]_C$ means that H_N and T must be diagrammatically connected. Substituting eq 1 into the Schrödinger equation and projecting it onto the determinant manifolds created by acting R on the reference $|\Phi\rangle$, we obtain

$$\langle\Omega|\bar{H}_N R|\Phi\rangle = (E_{corr} + \omega)\langle\Omega|R|\Phi\rangle \tag{7}$$

or

$$\langle\Omega|(\bar{H}_N R)_C|\Phi\rangle = \omega\langle\Omega|R|\Phi\rangle \tag{8}$$

to determine R and excitation energy ω, where E_{corr} is the correlation energy which can be calculated by

$$\langle\Phi|\bar{H}_N|\Phi\rangle = E_{corr} \tag{9}$$

Since $\bar{H}_N$ is non-Hermitian, it has distinct left- and right-hand-side eigenvectors. Both of them are needed for molecular properties, such as dipole moments and transition dipole moments. The L operator, which generates the left-hand-side eigenvectors of $\bar{H}_N$, is defined as

$$L = \sum_{n=0}^{m} L_n \tag{10a}$$

$$L_n = \left(\frac{1}{n!}\right)^2 l_{i_1\cdots i_n}^{a_1\cdots a_n} C^{i_1}\cdots C^{i_n} C_{a_n}\cdots C_{a_1} \tag{10b}$$

and satisfies the condition

$$\langle\Phi|L\bar{H}_N|\Omega\rangle = (E_{corr} + \omega)\langle\Phi|L|\Omega\rangle \tag{11}$$

or

$$\langle\Phi|(L\bar{H}_N)_L|\Omega\rangle = \omega\langle\Phi|L|\Omega\rangle \tag{12}$$

where $(L\bar{H}_N)_L$ means that L and $\bar{H}_N$ must be diagrammatically linked.

Once we have the biorthogonal left- and right-hand-side eigenvectors of $\bar{H}_N$, the dipole moments can be calculated by[10]

$$\langle d\rangle_{(k)} = \langle\Phi|L(k)[d\exp(T)]_C R(k)|\Phi\rangle \tag{13}$$

where d is a dipole operator, and transition dipole moments can be calculated by[10]

$$\langle dd\rangle_{(kl)} = \langle\Phi|L(k)[d\exp(T)]_C R(l)|\Phi\rangle \times \langle\Phi|L(l)[d\exp(T)]_C R(k)|\Phi\rangle \tag{14}$$

The dipole and transition dipole moments calculated by the EOM-CC approach, eqs 13 and 14, are identical to those by the CC LR theory in the FCI limit, while there can be subtle differences in the approximate calculations.[63]

The EE-EOM-CCSDT[20,23] and EE-EOM-CCSDTQ[37,38] methods are obtained by truncating eqs 3a, 4a, 5, and 10a after $n = 3$ and 4, i.e., by setting $m = 3$ and 4, respectively. In the active-space EE-EOM-CC methods, we restrict the T_3, T_4, R_3, R_4, L_3, and L_4 operators to their subsets defined

in terms of the active spin-orbitals. To do so, we partition all spin-orbitals into core, active occupied, active unoccupied, and virtual spin-orbitals. We designate core spin-orbitals by *i*, *j*, *k*, active occupied spin-orbitals by *I*, *J*, *K*, active unoccupied spin-orbitals by *A*, *B*, *C*, and virtual spin-orbitals by *a*, *b*, *c*. The core and active occupied orbitals are those that are occupied in reference wave function $|\Phi\rangle$, and the active space is chosen by the user at runtime.

The restricted R_3 operators can be defined by using the excitations in which at least one, two, or three occupied and unoccupied spin-orbitals are active, and they are designated by $r_3^{(1)}$, $r_3^{(2)}$, and $r_3^{(3)}$, respectively, and written as

$$r_3^{(1)} = \left(\frac{1}{6}\right)^2 r_{Abc}^{iJK} C^A C^b C^c C_K C_j C_i \tag{15}$$

$$r_3^{(2)} = \left(\frac{1}{6}\right)^2 r_{ABc}^{iJK} C^A C^B C^c C_K C_J C_i \tag{16}$$

and

$$r_3^{(3)} = \left(\frac{1}{6}\right)^2 r_{ABC}^{IJK} C^A C^B C^C C_K C_J C_I \tag{17}$$

The restricted T_3 ($\{t_3^{(i)}|1 \le i \le 3\}$), T_4 ($\{t_4^{(i)}|1 \le i \le 4\}$), R_4 ($\{r_4^{(i)}|1 \le i \le 4\}$), L_3 ($\{l_3^{(i)}|1 \le i \le 3\}$), and L_4 ($\{l_4^{(i)}|1 \le i \le 4\}$) operators are defined analogously.

Replacing T_3, R_3, and L_3 in the EE-EOM-CCSDT ansatz by $t_3^{(i)}$, $r_3^{(i)}$, and $l_3^{(i)}$, we obtain EE-EOM-CCSD*t* ($i = 1$),[22,23,45] EE-EOM-CCSD*t*(II) ($i = 2$),[45] and EE-EOM-CCSD*t*(III) ($i = 3$).[45] EE-EOM-CCSDT*q*, EE-EOM-CCSDT*q*(II), EE-EOM-CCSDT*q*(III), and EE-EOM-CCSDT*q*(IV) can likewise be defined by replacing T_4, R_4, and L_4 in the EOM-CCSDTQ equations by $t_4^{(i)}$, $r_4^{(i)}$, and $l_4^{(i)}$ ($1 \le i \le 4$), respectively. The use of $t_3^{(1)}$, $r_3^{(1)}$, $l_3^{(1)}$, $t_4^{(2)}$, $r_4^{(2)}$, and $l_4^{(2)}$ in EE-EOM-CCSDTQ leads to EE-EOM-CCSD*tq*.[22] Obviously, we can concoct many other variants by combining these active-space triples and quadruples in EE-EOM-CCSDTQ. For instance, with the use of $t_3^{(3)}$, $r_3^{(3)}$, $l_3^{(3)}$, $t_4^{(4)}$, $r_4^{(4)}$, and $l_4^{(4)}$, we arrive at a method that can be called EE-EOM-CCSD*t*(III)*q*(IV). If one active-space restriction is imposed on all of T_n, R_n, and L_n for a given rank *n*, the resulting method is size extensive and intensive. Equations 5, 8, and 12 with restricted T_n, R_n, and L_n ($n = 3,4$) and a manifold Ω with restricted triple and quadruple excitation determinants need to be solved to determine the unknown coefficients in these methods.

The IP- and EA-EOM-CC methods can be formulated by replacing the *R* operator and manifold $|\Omega\rangle$ in eqs 1, 7, and 8 by $R^{(N\mp1)}$, which are defined as

$$R^{(N-1)} = \sum_{n=1}^{m} R_n^{(N-1)} \tag{18}$$

$$R_n^{(N-1)} = \frac{1}{n!(n-1)!} r_{a_1 \cdots a_{n-1}}^{i_1 \cdots i_n} C^{a_1} \cdots C^{a_{n-1}} C_{i_n} \cdots C_{i_1} \tag{19}$$

and

$$R^{(N+1)} = \sum_{n=1}^{m} R_n^{(N+1)} \tag{20}$$

$$R_n^{(N+1)} = \frac{1}{n!(n-1)!} r_{a_1 \cdots a_n}^{i_1 \cdots i_{n-1}} C^{a_1} \cdots C^{a_n} C_{i_{n-1}} \cdots C_{i_1} \tag{21}$$

Accordingly, the manifolds $|\Omega^{(N-1)}\rangle$ and $|\Omega^{(N+1)}\rangle$ are spanned by $|\Phi_i\rangle$, $|\Phi_{ij}^a\rangle$, $|\Phi_{ijk}^{ab}\rangle$, etc., and $|\Phi^a\rangle$, $|\Phi_i^{ab}\rangle$, $|\Phi_{ij}^{abc}\rangle$, etc., respectively.

The IP/EA-EOM-CCSDT and IP/EA-EOM-CCSDTQ methods are defined by eqs 4, 5, 18, and 19 with $m = 3$, and 4, respectively. Their active-space variants restrict the T_3, T_4, $R_3^{(N\mp1)}$, and $R_4^{(N\mp1)}$ operators to their subsets. Since the $R_3^{(N\mp1)}$ operators have an unequal number of creation and annihilation operators, the restriction can be imposed in one of the following two ways

$$r_3^{(N-1),A,(1)} = \left(\frac{1}{12}\right) r_{Bc}^{ijK} C^B C^c C_K C_j C_i \tag{22}$$

or[47]

$$r_3^{(N-1),B,(1)} = \left(\frac{1}{12}\right) r_{bc}^{iJK} C^b C^c C_K C_j C_i \tag{23}$$

Likewise, the active-space $R_4^{(N-1)}$ operator can be either

$$r_4^{(N-1),A,(1)} = \left(\frac{1}{144}\right) r_{Bcd}^{ijkL} C^B C^c C^d C_L C_k C_j C_i \tag{24}$$

$$r_4^{(N-1),A,(2)} = \left(\frac{1}{144}\right) r_{BCd}^{ijKL} C^B C^C C^d C_L C_K C_j C_i \tag{25}$$

or

$$r_4^{(N-1),B,(1)} = \left(\frac{1}{144}\right) r_{bcd}^{ijkL} C^b C^c C^d C_L C_k C_j C_i \tag{26}$$

$$r_4^{(N-1),B,(2)} = \left(\frac{1}{144}\right) r_{Bcd}^{ijKL} C^B C^c C^d C_L C_K C_j C_i \tag{27}$$

The restricted $R_3^{(N+1)}$ and $R_4^{(N+1)}$ can be defined analogously.

Replacing T_3 by $t_3^{(1)}$ and $R_3^{(N\mp1)}$ by $r_3^{(N\mp1),A,(1)}$ ($r_3^{(N\mp1),B,(1)}$) in IP/EA-EOM-CCSDT leads to the IP/EA-EOM-CCSD*t*-A and -B methods, which have been proposed by Gour et al.[47] The IP/EA-EOM-CCSDT*q*-A and -B and IP/EA-EOM-CCSD*tq*-A and -B methods can also be defined completely analogously. The size dependence of the computational costs of the A variants is one-rank lower than that of the B counterparts in the step of solving $R^{(N\mp1)}$ (the common CCSD step incurs the same cost for both). Both methods are size extensive for total energies and intensive for transition energies.

III. Computer Implementation

In our previous report on the active-space CC methods for the ground state,[42] we described the salient modifications to the symbolic algebra system TCE needed for it to perform the automated formula derivation and computer implementation of these methods. One important feature of the TCE-synthesized programs is the tiling algorithm, which has also been proposed and implemented by Windus and Pople[64] as the "block-tensor" algorithm. In this algorithm, orbitals are grouped into tiles, and every tile is a set of orbitals which have the common attributes of hole/particle distinction, spatial symmetry, and spin symmetry. Once the tiles are defined, tensor contractions and additions can be carried out by the tilewise matrix multiplications and additions, taking account of the spin, spatial, and permutation symmetries.[51]

The TCE has been extended to handle various active-space ansatz by simply adding the active/inactive attribute to each tile.[42] In the TCE-synthesized EE-EOM-CCSD*t* program, for instance, the tiles of the amplitudes $t_3^{(1)}$ (t_{Abc}^{ijK}), $r_3^{(1)}$ (r_{Abc}^{ijK}), and $l_3^{(1)}$ (l_{ijK}^{Abc}) that are stored and used in contractions are limited to those that have at least one active particle tile index and at least one active hole tile index. The numbers of eqs 5, 7, and 11 are likewise reduced since only the tiles of triples excitations in Ω that have at least one active particle tile index and one active hole tile index are retained. Many tiles of intermediate quantities of active-space EE-EOM-CC calculations can also be excluded. Only those tiles that satisfy the universal formula, $n_B \geq n_C - n_D + n_A$, need to be considered, where n_B is the number of superscript (or subscript) active external indices in the intermediate (the external indices are the indices in Ω), n_C is equal to i in $t_n^{(i)}$, $r_n^{(i)}$, or $l_n^{(i)}$, n_D is the number of superscript (or subscript) external indices of Ω, and n_A is the number of superscript (or subscript) external indices in the intermediate.

The TCE has also been extended to handle the IP/EA-EOM-CC approaches through quadruples.[31,35] To allow the $R^{(N\mp1)}$ operators in the ansatz, we have added a new attribute to each of the creation and annihilation operators and each of the indices of physical tensors (molecular integrals, excitation amplitudes, and so forth), which distinguishes the usual operators and indices from those that are associated with a continuum operator. One additional rule is introduced: a continuum operator can only be contracted with another continuum operator,[31] when evaluating an expectation value of normal-ordered second-quantized operators using Wick's theorem. Once the active-space logic and the IP/EA extension are combined, the TCE can be used to generate the active-space IP/EA-EOM-CC codes as well as active-space EE-EOM-CC codes.

The EE-EOM-CCSD*t*, EE-EOM-CCSD*t*(II), and EE-EOM-CCSD*t*(III) methods have been implemented in a single algorithmic framework that switches among these three and also EE-EOM-CCSDT according to a runtime parameter set by the user of the program. The EE-EOM-CCSD*tq*, EE-EOM-CCSD*t*(I)*q*(III), EE-EOM-CCSD*t*(I)*q*(IV), EE-EOM-CCSD*t*(II)*q*(III), EE-EOM-CCSD*t*(II)*q*(IV), EE-EOM-CCSD*t*(III)*q*(IV), EE-EOM-CCSDT*q*, EE-EOM-CCSDT*q*(II), EE-EOM-CCSDT*q*(III), and EE-EOM-CCSDT*q*(IV) can also be executed by a single algorithm that also encompasses EE-EOM-CCSDTQ. The IP and EA variants, IP/EA-EOM-CCSD*t*-A and -B, IP/EA-EOM-CCSD*tq*-A and -B, and IP/EA-EOM-CCSDT*q*-A and -B, are implemented in the same fashion. When using the formula $n_B \geq n_C - n_D + n_A$, a continuum index can be either ignored altogether or counted as an active, external index toward n_B, n_D, and n_A. The former choice defines the A variant and the latter the B variant.

These programs are parallel executable on the basis of a distributed- or replicated-data, load-balancing algorithm, adjust tile sizes automatically according to the user specified memory limit, and make use of the spin (within spin-orbital formalisms), spatial (real Abelian), and permutation symmetries. They can be applied to atoms and molecules of any number of electrons and any spin multiplicity (with certain molecular size limits). They are a part of the NWChem computational chemistry program suite.[65]

The code verification has been done by the comparison with an independent implementation of the same methods using the determinant-based algorithm[56] for the right-hand-side eigenvalue problem. The TCE-synthesized codes for the left-hand-side eigenvalue problem have been verified to give the identical eigenvalues as the right-hand-side codes. We have observed the speedup by a factor of 10 and 3 for EE-EOM-CCSD*tq* and EE-EOM-CCSDT*q*, respectively, relative to EE-EOM-CCSDTQ, for the excitation energies of C_2 with a modified cc-pVDZ basis set.[66] The parallel algorithms employed here are unchanged from our prior studies,[37,42,45,51−54] and their performance can be inferred from the data given therein.[42,51,52]

Table 1. Vertical Excitation Energies (in eV) of C_2

theory	active space	$^1\Pi_u$	$^1\Delta_g$	$^1\Pi_g$	$^1\Sigma_u^+$
FCI[a]	···	1.385	2.293	4.494	5.602
EE-EOM-CCSD[b]	···	+0.090	+2.054	+1.708	+0.197
EE-EOM-CCSDT[b]	···	+0.034	+0.407	+0.088	+0.113
EE-EOM-CCSD*t*	(2,2)	−0.077	+0.244	+0.070	+0.123
EE-EOM-CCSD*t*	(2,7)	−0.038	+0.282	+0.063	+0.097
EE-EOM-CCSDTQ[b]	···	+0.001	+0.024	−0.007	+0.013
EE-EOM-CCSD*tq*	(2,2)	−0.083	−0.057	+0.065	+0.061
EE-EOM-CCSD*tq*	(2,7)	−0.056	−0.034	+0.027	+0.027
EE-EOM-CCSDT*q*	(2,2)	−0.004	+0.036	+0.007	+0.012
EE-EOM-CCSDT*q*	(2,7)	−0.002	+0.034	+0.001	+0.013
EE-EOM-CCSD*t*(EII)	(2,2)	−0.131	+1.527	+1.312	+0.204
EE-EOM-CCSD*t*(EIII)	(2,2)	+0.089	+2.054	+1.707	+0.197
EE-EOM-CCSD*t*(EI)*q*(III)	(2,2)	−0.077	+0.243	+0.070	+0.123
EE-EOM-CCSD*t*(EI)*q*(IV)	(2,2)	−0.077	+0.244	+0.070	+0.123
EE-EOM-CCSD*t*(EII)*q*(III)	(2,2)	−0.131	+1.526	+1.312	+0.204
EE-EOM-CCSD*t*(EII)*q*(IV)	(2,2)	−0.131	+1.527	+1.312	+0.204
EE-EOM-CCSD*t*(EIII)*q*(IV)	(2,2)	+0.089	+2.054	+1.707	+0.197
EE-EOM-CCSDT*q*(II)	(2,2)	+0.020	+0.118	+0.102	+0.047
EE-EOM-CCSDT*q*(III)	(2,2)	+0.034	+0.406	+0.088	+0.113
EE-EOM-CCSDT*q*(IV)	(2,2)	+0.034	+0.407	+0.088	+0.113

[a] Reference 66. [b] Reference 37.

IV. Applications

A. Vertical Excitation Energies of C_2. The active-space EE-EOM-CC results for C_2, a molecule notorious for the multideterminant ground-state wave function at the equilibrium geometry, are shown in Table 1. The FCI results[66] in this table are listed as the vertical excitation energies, while the other entries are the differences from the FCI. We have used 2.348 bohr[66] as the internuclear distance and the cc-pVDZ basis set[67] with an additional diffuse function for each valence orbital[66] in the frozen core approximation. Two types of active space have been used: the first selects the two highest occupied and two lowest unoccupied α- and β-spin orbitals as active orbitals. The second uses two active occupied and seven unoccupied α- and β-spin orbitals. We use "(2,2)" to designate the first and "(2,7)" the second active space.

Four low-lying excited states $^1\Pi_u$, $^1\Delta_g$, $^1\Pi_g$, and $^1\Sigma_u^+$ have been examined. The $^1\Delta_g$ and $^1\Pi_g$ states are dominated by doubly excited determinant contributions, noticeable by the significant improvement in excitation energies brought to by

Table 2. Adiabatic Excitation Energies (T_e/eV) and Dipole Moments (μ/D) of the Ground and Low-Lying Excited States of CH

	$\tilde{X}^2\Pi$		$\tilde{a}^4\Sigma^-$		$\tilde{A}^2\Delta$		$\tilde{B}^2\Sigma^-$		$\tilde{C}^2\Sigma^+$	
theory[a]	T_e	μ	T_e	μ	T_e	μ	T_e	μ	T_e	μ
CCSD/aug-cc-pVDZ[b]	0.00	1.39	0.95	0.65	3.33	0.81	4.41	0.91	5.29	0.72
CCSD/aug-cc-pVTZ[b]	0.00	1.42	1.03	0.65	3.28	0.81	4.62	0.90	5.48	0.71
CCSDT/aug-cc-pVDZ[b]	0.00	1.37	0.66	0.65	3.02	0.81	3.27	1.27	4.07	0.87
CCSD*t*/aug-cc-pVDZ	0.00	1.38	0.76	0.67	3.12	0.82	3.42	1.20	4.18	0.88
CCSDT/aug-cc-pVTZ[b]	0.00	1.39	0.74	0.65	2.94	0.81	3.27	1.27	4.03	0.87
CCSD*t*/aug-cc-pVTZ	0.00	1.41	0.86	0.66	3.07	0.82	3.50	1.17	4.19	0.88
CCSDTQ/aug-cc-pVDZ[b]	0.00	1.37	0.65	0.65	3.00	0.81	3.26	1.27	4.04	0.86
CCSD*tq*/aug-cc-pVDZ	0.00	1.38	0.76	0.67	3.12	0.82	3.42	1.20	4.17	0.88
CCSDT*q*/aug-cc-pVDZ	0.00	1.37	0.65	0.65	3.01	0.81	3.26	1.27	4.04	0.86
experiment	0.00	1.46 ± 0.06[c]	0.74[d]	⋯	2.88[e]	0.77 ± 0.07[f]	3.23[g]	⋯	3.94[e]	⋯

[a] CCSD represents CCSD for the ground state $\tilde{X}^2\Pi$ or EE-EOM-CCSD for the rest. Likewise, CCSDT, CCSDTQ, CCSD*t*, CCSD*tq*, and CCSDT*q* represent either the CC or EE-EOM-CC methods. [b] Reference 37. [c] Reference 73. [d] Reference 74. [e] Reference 72. [f] Reference 75. [g] Reference 71.

the inclusion of triples (EE-EOM-CCSDT). For $^1\Delta_g$, EE-EOM-CCSD*t* with (2,2) active space gives +0.244 eV difference from the FCI results. Hence, it is as accurate as EE-EOM-CCSDT, which suffers from the slightly greater error of +0.407 eV. EE-EOM-CCSD*tq* and EE-EOM-CCSDT*q* further reduce the deviations to −0.057 eV and +0.036 eV and rival EE-EOM-CCSDTQ in accuracy. We can make similar observations in the results of the $^1\Pi_g$ state. The $^1\Sigma_u^+$ and $^1\Pi_u$ states are approximated by single determinants, and only marginal (< 0.1 eV) improvements relative to EE-EOM-CCSD are obtainable by EE-EOM-CCSDT. For the $^1\Sigma_u^+$ state, in particular, EE-EOM-CCSD*t*, EE-EOM-CCSD*tq*, and EE-EOM-CCSDT*q* all exhibit rapid convergence to the FCI results.

When the active space is extended to (2,7), all of the results of the active-space methods improve. However, the improvement is very small and in the order of 0.01 eV for the EE-EOM-CCSD*t* and EE-EOM-CCSD*tq* methods, and in the order of 0.001 eV for the EE-EOM-CCSDT*q* method, attesting to the effectiveness of the active-space methods with a minimum active space.

We have also examined the relative performance of various definitions of active-space triples and quadruples with active space (2,2). The EE-EOM-CCSD*t*(III) energies constitute no improvement over the EE-EOM-CCSD ones, while the EE-EOM-CCSD*t*(II) energies are in marginally closer agreement to the FCI values by 0.4−0.5 eV for excited states with two-electron character. This indicates that the use of "*t*(I)=*t*" ansatz for active-space triples is essential as "*t*(II)" can capture too small a portion of significant triples contributions and "*t*(III)" is even less meaningful. EE-EOM-CCSD*t*(I)-*q*(III), EE-EOM-CCSD*t*(II)*q*(III), EE-EOM-CCSD*t*(III)*q*(III), and EE-EOM-CCSDT*q*(III) simply reproduce the results of EE-EOM-CCSD*t*(I)=EE-EOM-CCSD*t*, EE-EOM-CCSD*t*(II), EE-EOM-CCSD*t*(III), and EE-EOM-CCSDT, respectively. The "*q*(III)" and hence also "*q*(IV)" variants of active-space quadruples are inadequate. The "*q*(II)" is the crudest meaningful approximation and is employed in EE-EOM-CCSD*tq*. The effectiveness of "*q*(I)=*q*" in EE-EOM-CCSDT*q* is already emphasized (see above).

B. Adiabatic Excitation Energies and Dipole Moments of the CH Radical. Table 2 compiles the adiabatic excitation energies and dipole moments of low-lying excited states ($\tilde{a}^4\Sigma^-$, $\tilde{A}^2\Delta$, $\tilde{B}^2\Sigma^-$, and $\tilde{C}^2\Sigma^+$) of the CH radical. We have used the aug-cc-pVDZ and aug-cc-pVTZ[67,68] basis sets with the frozen core approximation. The equilibrium bond lengths have been taken from experiment, and they are 1.1197868 Å,[69] 1.0977 Å,[70] 1.1031 Å,[69] 1.1640 Å,[71] and 1.1143 Å[72] for states $\tilde{X}^2\Pi$, $\tilde{a}^4\Sigma^-$, $\tilde{A}^2\Delta$, $\tilde{B}^2\Sigma^-$, and $\tilde{C}^2\Sigma^+$, respectively. The active space adopted is minimum, consisting of (2,2) for the α-spin orbitals and (1,3) for the β-spin orbitals. The symmetries of the active-space orbitals are a_1, b_2, b_1, and a_1 for α-spin orbitals and a_1, b_1, a_1, and b_2 for β-spin orbitals. The experimental values of excitation energies and dipole moments have been taken from refs 71−75.

For the $\tilde{a}^4\Sigma^-$ and $\tilde{A}^2\Delta$ states, the differences in excitation energies between EE-EOM-CCSD and EE-EOM-CCSDT are about 0.3 eV. EE-EOM-CCSD*t* yields the excitation energy within 0.1 eV of EE-EOM-CCSDT, recovering only $^2/_3$ of the contribution due to triples. The effect of quadruples is minimal, which is in the order of 0.01 eV. The marked decrease in the effectiveness of EE-EOM-CCSD*t* for these states is ascribed to the fact that the triples effects are better described as dynamical correlation, unsuitable to be treated by active-space triples. The dipole moments of these states obtained from EE-EOM-CCSD, EE-EOM-CCSDT, and EE-EOM-CCSDTQ are essentially identical. There is no indication that the active-space methods introduce significant errors. The accurate agreement between EE-EOM-CCSD*t*/aug-cc-pVDZ or EE-EOM-CCSD*tq*/aug-cc-pVDZ and experiment[74] is fortuitous.

In the excitation energies to the $\tilde{B}^2\Sigma^-$ and $\tilde{C}^2\Sigma^+$ states, the triples effects reach more than 1 eV, reflecting greater two-electron character of these states. The deviation between EE-EOM-CCSD*t* and EE-EOM-CCSDT is about 0.15 eV, and the former captures 88% of correlation due to triples. For $\tilde{C}^2\Sigma^+$, the deviation is 0.11 eV, and EE-EOM-CCSD*t* recovers 91% of correlation due to triples. Generally, the EE-EOM-CCSD*t* with an adequate minimum active space seems capable of exhausting nondynamical correlation due to triples (e.g., associated with two-electron character in excited states), leaving only dynamical correlation due to triples on the order of 0.1−0.2 eV with aug-cc-pVDZ for this molecule. The inclusion of active-space triples clearly

Table 3. Adiabatic Excitation Energies (T_e/eV) and Dipole Moments (μ/D) of the Ground State and the Lowest-Lying Singlet Excited State of Formaldehyde

state	theory	T_e	μ
$^1A_1$	CCSD/aug-cc-pVDZ[a]	0.00	2.34
	CCSD/aug-cc-pVTZ[a]	0.00	2.38
	CCSDT/aug-cc-pVDZ[a]	0.00	2.33
	CCSD*t*/aug-cc-pVDZ	0.00	2.34
	Experiment	0.00	2.33[b]
$^1A_2$	EE-EOM-CCSD/aug-cc-pVDZ[a]	3.64	1.28
	EE-EOM-CCSD/aug-cc-pVTZ[a]	3.73	1.27
	EE-EOM-CCSDT/aug-cc-pVDZ[a]	3.49	1.48
	EE-EOM-CCSD*t*/aug-cc-pVDZ	3.49	1.43
	experiment	3.49[c]	1.56 ± 0.07[d]

[a] Reference 37. [b] Reference 77. [c] Reference 78. [d] Reference 79.

leads to improved agreement between calculated and observed[71,72] excitation energies of these states.

When the basis set size is increased to aug-cc-pVTZ, EE-EOM-CCSD*t* becomes slightly less effective. For $\tilde{B}^2\Sigma^-$ and $\tilde{C}^2\Sigma^+$, the differences between EE-EOM-CCSD*t* and EE-EOM-CCSDT are 0.23 and 0.16 eV, respectively, with the active-space triples recovering 83 and 89% of correlation due to all triples. A similar observation can be made for active-space quadruples. This may be explained as follows. The greater fidelity in describing the dynamical correlation effects (but not necessarily the nondynamical ones) is afforded by larger basis sets. Hence the increase in basis set size widens the gap between the conventional method and its active-space counterparts, as the latter are limited in capturing dynamical correlation due to triples (and/or quadruples).

There are significant differences between EE-EOM-CCSD and EE-EOM-CCSDT in the dipole moments of the $\tilde{B}^2\Sigma^-$ and $\tilde{C}^2\Sigma^+$ states. They amount to 0.36 and 0.15 D, respectively. On the other hand, no difference can be seen between the EE-EOM-CCSDT and EE-EOM-CCSDTQ values. EE-EOM-CCSD*t* reduces these differences to 0.07 and 0.01 D for the $\tilde{B}^2\Sigma^-$ and $\tilde{C}^2\Sigma^+$ states with the aug-cc-pVDZ basis set and 0.1 and 0.01 D with the aug-cc-pVTZ basis set. The higher-order active-space EE-EOM-CC methods display equal (or even greater) effectiveness in recovering correlation effects on the excited-state dipole moments.

C. Adiabatic Excitation Energies and Dipole Moments of Formaldehyde. Next we examine the dipole moment of the ground ($^1A_1$) state and the adiabatic excitation energy and dipole moment of the lowest-lying excited ($^1A_2$) state of formaldehyde (Table 3). The planar equilibrium geometry of the ground state $^1A_1$ is r_{CH} = 1.116 Å, r_{CO} = 1.208 Å, and a_{HCH} = 116.5°,[76] and the nonplanar equilibrium geometry of the $^1A_2$ state is r_{CH} = 1.103 Å, r_{CO} = 1.323 Å, a_{HCH} = 118.1°, and CH_2 out-of-plane angle = 34.0°.[76] We have chosen (3,2) active space, and the frozen core approximation has been used. The symmetries of the active-space orbitals are a_1, b_1, b_2, a_1, and b_2 for the planar geometry and a', a', a'', a', and a' for the nonplanar geometry.

For the ground state, the CCSD and CCSDT dipole moments agree within 0.01 D, and the triples effect is essentially null. The CCSD*t* result is within 0.01 D of these two values and also of the experimental finding (2.33 D).[77] The adiabatic excitation energy to the $^1A_2$ undergoes a decrease of 0.15 eV upon inclusion of the triples by EE-EOM-CCSDT. EE-EOM-CCSD*t* recovers this downward shift accurately, which may indicate that this is caused by nondynamical correlation or the rearrangement of electrons in the active space. Although the basis set effect is still significant, the closer agreement between EE-EOM-CCSDT or EE-EOM-CCSD*t* and experiment (3.49 eV)[78] than EE-EOM-CCSD is meaningful. The excited-state dipole moment also increases from 1.28 to 1.48 D on going from EE-EOM-CCSD to EE-EOM-CCSDT. The EE-EOM-CCSD*t* predicts 1.43 D, recovering 3/4 of the triples effect, and in much closer agreement with experiment (1.56 ± 0.07D).[79]

Table 4. Adiabatic Excitation Energies (in eV) to Low-Lying Excited States of the CH_2[a]

theory[b]	$\tilde{a}^1A_1$	$\tilde{b}^1B_1$	$\tilde{c}^1A_1$
EE-EOM-CCSD/aug-cc-pVDZ	0.48	1.57	3.72
EE-EOM-CCSDT/aug-cc-pVDZ	0.43	1.54	2.65
EE-EOM-CCSD*t*/aug-cc-pVDZ	0.45	1.56	2.81
EE-EOM-CCSDTQ/aug-cc-pVDZ	0.43	1.54	2.67
EE-EOM-CCSD*tq*/aug-cc-pVDZ	0.45	1.56	2.83
EE-EOM-CCSDT*q*/aug-cc-pVDZ	0.43	1.54	2.68
EE-EOM-CCSD/aug-cc-pVTZ	0.46	1.46	3.89
EE-EOM-CCSDT/aug-cc-pVTZ	0.41	1.43	2.53
EE-EOM-CCSD*t*/aug-cc-pVTZ	0.43	1.44	2.79

[a] The ground state is $\tilde{X}^3B_1$. [b] The EE-EOM-CC methods represent the corresponding CC methods for the $\tilde{a}^1A_1$ state.

D. Adiabatic Excitation Energies of CH_2. Some of the low-lying singlet states of CH_2 are said to have diradical character,[80−83] which warrants a high-order CC description. We have calculated the adiabatic excitation energies to the $\tilde{a}^1A_1$, $\tilde{b}^1B_1$, and $\tilde{c}^1A_1$ states from the ground $\tilde{X}^3B_1$ state, which requires the methods that can handle transitions from open to closed shells such as the spin-orbital EE-EOM-CC methods developed in this work (Table 4). The geometries used are r_e = 1.0775 Å, θ_e = 133.29° ($\tilde{X}^3B_1$); r_e = 1.1089 Å, θ_e = 101.89° ($\tilde{a}^1A_1$); r_e = 1.0748 Å, θ_e = 141.56° ($\tilde{b}^1B_1$); r_e = 1.0678 Å, θ_e = 170.08° ($\tilde{c}^1A_1$).[83] The aug-cc-pVDZ and aug-cc-pVTZ basis sets[67,68] have been used with the frozen core approximation. The active spaces are (2,3) for the singlet states and (3,2) for the α-spin orbitals and (1,4) for the β-spin orbitals of the triplet state. The symmetries of the active-space orbitals are b_2, a_1, b_1, a_1, and b_2 for the singlet states and b_2, a_1, b_1, a_1, and b_2 for α-spin orbitals and b_2, a_1, b_2, a_1, and b_1 for β-spin orbitals of the triplet state.

The singlet−triplet separation of CH_2, i.e., the energy difference between the $\tilde{a}^1A_1$ and $\tilde{X}^3B_1$ states, has been used to assess the accuracy of theoretical methods.[81,84−86] These studies showed that CCSDT or its perturbative approximation CCSD(T) is the minimum level of theory for its quantitative description. Previously, we demonstrated that the CCSD*t* method with (3,3) or (2,2) active space is another inexpensive alternative to CCSDT with only a small penalty in accuracy (within 0.2 kcal/mol).[42] The results in Table 4 reiterate the importance of the triples effect in the splitting in which the difference between CCSD and CCSDT is approximately −0.05 eV. However, unlike our previous CCSD*t* work,

CCSD*t*/aug-cc-pV*n*Z with (2,3) active space captures only 60% of the triples effect as opposed to 80−90% by CCSD*t*/cc-pV*n*Z with (3,3) or (2,2) active space.[42] We have confirmed that this varied performance is simply the consequence of the diffuse functions of aug-cc-pV*n*Z basis sets that tend to make the low-lying unoccupied orbitals less suitable for active orbitals.

The $\tilde{b}^1B_1$ state is dominated by a single determinant, and hence the difference between EE-EOM-CCSD and EE-EOM-CCSDT in the excitation energy is less than 0.03 eV. The active-space methods nevertheless reduce the error but only slightly to 0.01−0.02 eV. The $\tilde{c}^1A_1$ state, on the other hand, can be viewed as a diradical, and the EE-EOM-CCSD excitation energy has an error in excess of 1 eV, which is characteristic of severe multideterminant character in the wave function. EE-EOM-CCSD*t* reduces this large error to mere 0.16 eV with the aug-cc-pVDZ basis set and to 0.26 eV with the aug-cc-pVTZ basis set. This also suggests that again the effectiveness of the active-space diminishes with increasing basis set sizes, and the remaining dynamical correlation on the order of 0.1−0.3 eV needs to be accounted for by other means. The quadruple effect is small and is about 0.02 eV. EE-EOM-CCSDT*q* can capture half of it.

E. Dissociation of Hydrogen Fluoride in the Excited $^1A_1$ State. One of the weaknesses of the active-space methods identified above is that its effectiveness declines with increasing basis set sizes. A larger basis set allows the nonactive-space methods to capture a greater proportion of dynamical correlation, but it does not benefit the active-space methods with fixed active-space sizes. Furthermore, the larger the basis set, the low-lying unoccupied orbitals become more diffuse, planewave-like, and less suitable as active orbitals. A remedy to this problem is to (variationally) optimize the orbitals in the active space, and such approaches in the context of CC theory have been reported, e.g., by Sherrill et al.[60] and by Krylov et al.[61,62]

We propose a much simpler alternative of using a multiresolution composite method[86] which combines higher-rank active-space methods with smaller basis sets for nondynamical correlation and lower-rank nonactive-space methods with larger basis sets for dynamical correlation. This not only circumvents the undesirable basis-set dependence of the active-space methods but also reduces the overall computational cost. We apply the scheme to bond breaking of hydrogen fluoride in the first excited ($^1A_1$) state, where the multideterminant effect is again prominent. The following formula has been used to approximate the total energy

$$E = E_{\mathrm{CIS}}(5\mathrm{Z}) + [E_{\mathrm{CCSD}}(\mathrm{QZ}) - E_{\mathrm{CIS}}(\mathrm{QZ})] + [E_{\mathrm{CCSD}t}(\mathrm{TZ}) - E_{\mathrm{CCSD}}(\mathrm{TZ})] + [E_{\mathrm{CCSD}tq}(\mathrm{DZ}) - E_{\mathrm{CCSD}t}(\mathrm{DZ})] \quad (28)$$

where subscripts and parentheses indicate the method (CCSD, CCSD*t*, etc. are understood to stand for EE-EOM-CCSD, EE-EOM-CCSD*t*, etc.) and basis sets (the cc-pV*n*Z series) with which individual energy components are computed. The active space consists of (3,1). The symmetries of the active-space orbitals are a_1, b_1, b_2, and a_1 at bond length of 2.0 bohr and b_2, b_1, a_1, and a_1 at bond lengths in the range of 3.0−9.0 bohr. The active space is essentially unchanged with bond lengths.

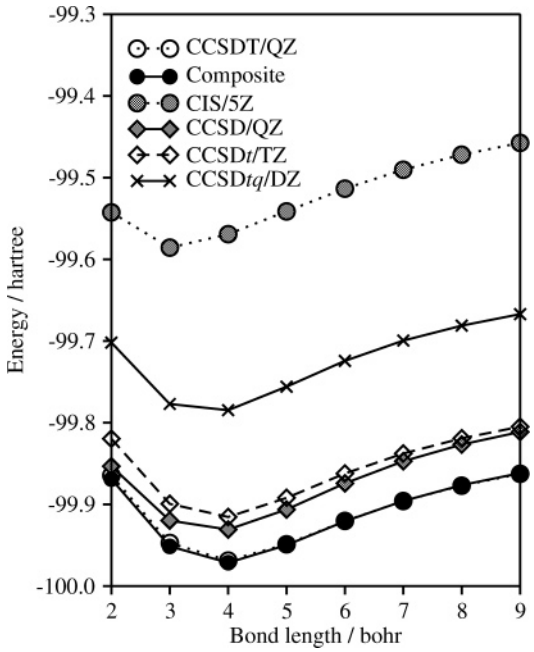

Figure 1. The energies of hydrogen fluoride in the first excited ($^1A_1$) state as a function of bond length. The CCSD, CCSD*t*, etc. label the corresponding EE-EOM-CC calculations and the composite calculations are based on eq 28.

The potential energy curves obtained by this composite method as well as by some of its components are depicted in Figure 1. The accuracy of the composite method rivals that of the EE-EOM-CCSDT/cc-pVQZ method, which is considerably more expensive than the composite method, as attested by the close agreement between the two curves. It is also noticed that none of the energy components is remotely as close to the EE-EOM-CCSDT/cc-pVQZ curve as their composite. For instance, the deviation between EE-EOM-CCSD/cc-pVQZ, which is the best performing component in eq 28, and EE-EOM-CCSDT/cc-pVQZ ranges between 11 and 51 mE_h, while that between the composite method and EE-EOM-CCSDT/cc-pVQZ is no more than 5 mE_h anywhere. In addition, the EE-EOM-CCSD/cc-pVQZ curve is clearly nonparallel to the EE-EOM-CCSDT/cc-pVQZ curve at shorter bond lengths, which is not the case with the curve obtained by the composite method. These results support the tacit assumption underlying this method that the basis-set dependence of nondynamical correlation is small and the dynamical and nondynamical correlation energies are separable.

F. Vertical Ionization Energies of N_2. The performance of the active-space IP-EOM-CC methods has been assessed by the calculation of the vertical ionization energies of N_2 (refs 30 and 31) (Table 5). The equilibrium bond distance 1.097685 Å has been taken from ref 72. The active space is (3,3), and the frozen core approximation has been used. The symmetries of the active-space orbitals are a_1, b_2, b_1, b_1, b_2, and a_1.

The $\tilde{X}^2\Sigma_g^+$, $\tilde{A}^2\Pi_u$, and $\tilde{B}^2\Sigma_u^+$ states of N_2^+ are the so-called Koopmans states, and the IP-EOM-CCSD descriptions are already accurate. The contributions of triples (quadruples) with the cc-pVDZ basis set are −0.08 eV (−0.04 eV), −0.29 eV (−0.01 eV), and −0.11 eV (−0.08 eV), respectively, in

Table 5. Vertical Ionization Energies (in eV) of N_2

theory	$\tilde{X}^2\Sigma_g^+$	$\tilde{A}^2\Pi_u$	$\tilde{B}^2\Sigma_u^+$	$\tilde{C}^2\Sigma_u^+$
IP-EOM-CCSD/cc-pVDZ	15.18	16.93	18.47	28.78
IP-EOM-CCSDT/cc-pVDZ	15.10	16.64	18.36	25.28
IP-EOM-CCSD*t*-A/cc-pVDZ	15.13	16.66	18.42	25.74
IP-EOM-CCSD*t*-B/cc-pVDZ	15.07	16.61	18.33	25.24
IP-EOM-CCSDTQ/cc-pVDZ	15.06	16.63	18.28	24.99
IP-EOM-CCSD*tq*-A/cc-pVDZ	15.10	16.66	18.35	25.60
IP-EOM-CCSD*tq*-B/cc-pVDZ	15.03	16.60	18.26	24.99
IP-EOM-CCSDT*q*-A/cc-pVDZ	15.06	16.63	18.28	25.04
IP-EOM-CCSDT*q*-B/cc-pVDZ	15.06	16.63	18.28	24.99
IP-EOM-CCSD/cc-pVTZ	15.56	17.18	18.83	29.50
IP-EOM-CCSDT/cc-pVTZ	15.44	16.90	18.67	25.63
IP-EOM-CCSD*t*-A/cc-pVTZ	15.54	16.98	18.81	26.42
IP-EOM-CCSD*t*-B/cc-pVTZ	15.38	16.83	18.61	25.53
IP-EOM-CCSD/cc-pVQZ	15.68	17.28	18.94	29.71
IP-EOM-CCSDT/cc-pVQZ	15.55	16.99	18.77	25.76
IP-EOM-CCSD*t*-A/cc-pVQZ	15.66	17.10	18.93	26.73
IP-EOM-CCSD*t*-B/cc-pVQZ	15.47	16.90	18.70	25.63

Table 6. Vertical Electron Affinities (in eV) of C_2

theory	$\tilde{X}^2\Sigma_g^+$	$\tilde{B}^2\Sigma_u^+$	$\tilde{A}^2\Pi_u$
EA-EOM-CCSD/aug-cc-pVDZ	3.13	−1.64	−0.43
EA-EOM-CCSDT/aug-cc-pVDZ	3.00	0.62	1.84
EA-EOM-CCSD*t*-A/aug-cc-pVDZ	2.87	0.54	1.90
EA-EOM-CCSD*t*-B/aug-cc-pVDZ	2.87	0.57	1.93
EA-EOM-CCSDTQ/aug-cc-pVDZ	3.00	0.74	2.28
EA-EOM-CCSD*tq*-A/aug-cc-pVDZ	2.88	0.46	2.17
EA-EOM-CCSD*tq*-B/aug-cc-pVDZ	2.88	0.50	2.21
EA-EOM-CCSDT*q*-A/aug-cc-pVDZ	3.00	0.71	2.26
EA-EOM-CCSDT*q*-B/aug-cc-pVDZ	3.00	0.71	2.26
EA-EOM-CCSD/aug-cc-pVTZ	3.30	−1.39	−0.63
EA-EOM-CCSDT/aug-cc-pVTZ	3.17	0.69	1.95
EA-EOM-CCSD*t*-A/aug-cc-pVTZ	2.99	0.61	2.05
EA-EOM-CCSD*t*-B/aug-cc-pVTZ	3.00	0.64	2.08
EA-EOM-CCSD/aug-cc-pVQZ	3.35	−1.22	−0.69
EA-EOM-CCSDT/aug-cc-pVQZ	3.21	0.72	1.97
EA-EOM-CCSD*t*-A/aug-cc-pVQZ	3.02	0.63	2.07
EA-EOM-CCSD*t*-B/aug-cc-pVQZ	3.01	0.66	2.11

the three states. The IP-EOM-CCSD*t*-A method captures a respectable portion of the triples, which are −0.05 eV, −0.27 eV, and −0.05 eV. The IP-EOM-CCSD*t*-B variant seems to work slightly better, although it tends to overshoot the triples contributions by 0.03 eV, at a significantly higher computational cost. Both IP-EOM-CCSDT*q*-A and -B reproduce the IP-EOM-CCSDTQ results. IP-EOM-CCSD*tq*-A and -B are equally effective in capturing the quadruples effects, but they retain the errors caused by the active-space treatment of triples. When the basis set is extended to cc-pVTZ and cc-pVQZ, IP-EOM-CCSD*t*-A approaches IP-EOM-CCSD in its performance, and IP-EOM-CCSD*t*-B becomes increasingly superior to IP-EOM-CCSD*t*-A as the latter adopts the more compact $R^{(N-1)}$ operator.

The $\tilde{C}^2\Sigma_u^+$ state is the destination of a satellite ionization transition with substantial triples effects, which amount to +3.50 eV, +3.87 eV, and +3.95 eV according to the calculations with the cc-pVDZ, cc-pVTZ, and cc-pVQZ basis sets, respectively. Both IP-EOM-CCSD*t*-A and -B methods capture a majority of the triples contributions, while the B variant is again distinctly superior to the A counterpart. With cc-pVDZ, IP-EOM-CCSD*t*-A is in error (from IP-EOM-CCSDT) by +0.46 eV, whereas IP-EOM-CCSD*t*-B is by only −0.04 eV. With larger basis sets, the gap in performance between the A and B variants widens. Essentially the same observation can be made for the active-space quadruples contributions. IP-EOM-CCSD*tq*-A incurs the error of +0.61 eV from IP-EOM-CCSDTQ, which can be minimized by IP-EOM-CCSD*tq*-B to 0.01 eV.

G. Vertical Electron Affinities of C_2. The electron affinities of C_2 pose perhaps the severest multideterminant problem for the EA-EOM-CC methods. The EA-EOM-CCSD method is known to predict incorrectly that the two lowest-lying excited states ($\tilde{A}^2\Pi_u$ and $\tilde{B}^2\Sigma_u^+$) of C_2^- are unstable toward autoionization and C_2^- can exist only in the ground state ($\tilde{X}^2\Sigma_g^+$).[35] In Table 6, we have compiled the active-space EA-EOM-CC results of the vertical electron affinities of C_2 computed at the equilibrium bond distance 1.243 Å (ref 72) with the aug-cc-pVDZ, aug-cc-pVTZ, and aug-cc-pVQZ basis sets and the frozen core approximation. The active space is (3,3). The symmetries of the active-space orbitals are a_u, b_u, b_u, a_g, a_u, and b_g for the aug-cc-pVDZ basis set and a_u, b_u, b_u, a_g, a_u, and a_g for aug-cc-pVTZ and QZ basis sets.

The electron affinity associated with the $\tilde{X}^2\Sigma_g^+$ state can be predicted reasonably accurately by either EA-EOM-CCSD or EA-EOM-CCSDT. Both EA-EOM-CCSD*t*-A and -B overshoot the triples effects. Consequently they do not necessarily reduce the differences in the electron affinity between EA-EOM-CCSD from EA-EOM-CCSDT, which are in the range of 0.13−0.14 eV. Again, this is because the active-space methods are not effective for dynamical correlation, which seems to constitute the majority of the triples effects of this state. The quadruples contribution in the electron affinity of this state is virtually null.

In the $\tilde{B}^2\Sigma_u^+$ state, the differences between EA-EOM-CCSD and EA-EOM-CCSDT are substantial, reaching 2.26 eV. The active-space methods reduce these differences to mere −0.09 eV (EA-EOM-CCSD*t*-A) and −0.06 eV (EA-EOM-CCSD*t*-B). The quadruples effect is relatively small, which is 0.12 eV, and the EA-EOM-CCSD*tq*-A and -B variants are not particularly useful. EA-EOM-CCSDT*q*-A and -B, however, reproduce EA-EOM-CCSDTQ within just 0.03 eV. A similar observation can be made to the $\tilde{A}^2\Pi_u$ state, except that the quadruples effect is more significant and amounts to 0.44 eV. EA-EOM-CCSD*tq*-A and -B capture 0.33 and 0.37 eV of this effect, respectively, which are about 80% of the quadruples effect. EA-EOM-CCSDT*q*-A and -B recover 0.42 eV or 95%.

V. Concluding Remarks

We have implemented and tested a wide range of approximations in the category of high-order active-space EOM-CC. They contain cluster and linear operators through quadruples for excited states, through four-hole-three-particle for ionized states, and through four-particle-three-hole for electron-attached states. The methods that include active-space triples of the type *t*(I)=*t* and/or active-space quadruples

of the type $q(\mathrm{I})=q$ or $q(\mathrm{II})$ can reproduce the corresponding nonactive-space EE/IP/EA-EOM-CC methods for dominantly two-electron or higher-order transitions. The use of minimum active spaces in EE/IP/EA-EOM-CCSD*t*, EE/IP/EA-EOM-CCSD*tq*, or EE/IP/EA-EOM-CCSDT*q* leads to accurate predictions for energies and related one-electron properties at a fraction of computational cost required in EE/IP/EA-EOM-CCSDT or EE/IP/EA-EOM-CCSDTQ. This article presents the most comprehensive exposition of this class of methods and their performance assessment, made possible by computerized symbolic algebra automating the formula derivation and implementations of the methods.

The active-space methods are found to be not as effective for the states that are already describable by EE/IP/EA-EOM-CCSD (e.g., within 0.1 eV of EE/IP/EA-EOM-CCSDT), where the triples effects are dynamical correlation. In a related note, the performance of the active-space methods gradually deteriorates with increasing basis set sizes. With a larger basis set, low-lying unoccupied orbitals become diffuse, planewave-like, and inadequate for active space. This undesirable basis-set dependence constitutes the most serious weakness of the active-space methods in the absence of any provision to optimize them such as those reported in refs 60−62. In this article, we have proposed and examined a much simpler alternative of using different basis sets for different methods or energy components. Our calculations on excited-state potential energy curves of hydrogen fluoride have demonstrated that nondynamical correlation effects can be isolated and are less sensitive to basis set sizes and can be described separately by the active-space methods with relatively small basis sets, while the dynamical correlation effects are treated by nonactive-space methods with more extensive basis sets.

Acknowledgment. This work has been supported by the National Science Foundation (CHE 0450462) and by the U.S. Department of Energy, Office of Basic Energy Sciences (DE-FG02-04ER15621). Some calculations were performed by using the Molecular Science Computing Facility in the William R. Wiley Environmental Molecular Sciences Laboratory, a national scientific user facility sponsored by the U.S. Department of Energy's Office of Biological and Environmental Research and located at the Pacific Northwest National Laboratory, operated for the Department of Energy by Battelle.

References

(1) Coester, F. *Nucl. Phys.* **1958**, *7*, 421.

(2) Coester, F.; Kümmel, H. *Nucl. Phys.* **1960**, *17*, 477.

(3) Čížek, J. *J. Chem. Phys.* **1966**, *45*, 4256.

(4) Čížek, J. *Adv. Chem. Phys.* **1969**, *14*, 35.

(5) Emrich, K. *Nucl. Phys. A* **1981**, *351*, 379.

(6) Emrich, K. *Nucl. Phys. A* **1981**, *351*, 397.

(7) Sekino, H.; Bartlett, R. J. *Int. J. Quantum Chem. Symp.* **1984**, 18, 255.

(8) Geertsen, J.; Rittby, M.; Bartlett, R. J. *Chem. Phys. Lett.* **1989**, *164*, 57.

(9) Comeau, D. C.; Bartlett, R. J. *Chem. Phys. Lett.* **1993**, *207*, 414.

(10) Stanton, J. F.; Bartlett, R. J. *J. Chem. Phys.* **1993**, *98*, 7029.

(11) Monkhorst, H. J. *Int. J. Quantum Chem. Symp.* **1977**, *11*, 421.

(12) Ghosh, S.; Mukherjee, D.; Bhattacharyya, S. *Mol. Phys.* **1981**, 43, 173.

(13) Dalgaard, E.; Monkhorst, H. J. *Phys. Rev. A* **1983**, *28*, 1217.

(14) Takahashi, M.; Paldus, J. *J. Chem. Phys.* **1986**, *85*, 1486.

(15) Koch, H.; Jørgensen, P. *J. Chem. Phys.* **1990**, *93*, 3333.

(16) Koch, H.; Jensen, H. J. A.; Jørgensen, P.; Helgaker, T. *J. Chem. Phys.* **1990**, *93*, 3345.

(17) Rico, R. J.; Head-Gordon, M. *Chem. Phys. Lett.* **1993**, *213*, 224.

(18) Nakatsuji, H.; Hirao, K. *Int. J. Quantum Chem.* **1981**, *20*, 1301.

(19) Nakatsuji, H.; Ohta, K.; Hirao, K. *J. Chem. Phys.* **1981**, *75*, 2952.

(20) Kucharski, S. A.; Włoch, M.; Musiał, M.; Bartlett, R. J. *J. Chem. Phys.* **2001**, *115*, 8263.

(21) Watts, J. D.; Bartlett, R. J. *J. Chem. Phys.* **1994**, *101*, 3073.

(22) Kowalski, K.; Piecuch, P. *J. Chem. Phys.* **2000**, *113*, 8490.

(23) Kowalski, K.; Piecuch, P. *J. Chem. Phys.* **2001**, *115*, 643.

(24) Piecuch, P.; Bartlett, R. J. *Adv. Quantum Chem.* **1999**, *34*, 295.

(25) Del Bene, J. E.; Watts, J. D.; Bartlett, R. J. *J. Chem. Phys.* **1997**, *106*, 6051.

(26) Nooijen, M.; Snijders, J. G. *Int. J. Quantum Chem. Symp.* **1992**, *26*, 55.

(27) Nooijen, M.; Snijders, J. G. *Int. J. Quantum Chem.* **1993**, *48*, 15.

(28) Stanton, J. F.; Gauss, J. *J. Chem. Phys.* **1994**, *101*, 8938.

(29) Stanton, J. F.; Gauss, J. *J. Chem. Phys.* **1994**, *111*, 8785.

(30) Musiał, M.; Kucharshi, S. A.; Bartlett, R. J. *J. Chem. Phys.* **2003**, *118*, 1128.

(31) Kamiya, M.; Hirata, S. *J. Chem. Phys.* **2006**, *125*, 074111.

(32) Nooijen, M.; Bartlett, R. J. *J. Chem. Phys.* **1995**, *102*, 3629.

(33) Nooijen, M.; Bartlett, R. J. *J. Chem. Phys.* **1995**, *102*, 6735.

(34) Musiał, M.; Bartlett, R. J. *J. Chem. Phys.* **2003**, *119*, 1901.

(35) Kamiya, M.; Hirata, S. *J. Chem. Phys.* **2007**, in press.

(36) Musiał, M.; Bartlett, R. J. *Chem. Phys. Lett.* **2004**, *384*, 210.

(37) Hirata, S. *J. Chem. Phys.* **2004**, *121*, 51.

(38) Kállay, M.; Gauss, J. *J. Chem. Phys.* **2004**, *121*, 9257.

(39) Oliphant, N.; Adamowicz, L. *Int. Rev. Phys. Chem.* **1993**, *12*, 339.

(40) Piecuch, P.; Oliphant, N.; Adamowicz, L. *J. Chem. Phys.* **1993**, 99, 1875.

(41) Piecuch, P.; Adamowicz, L. *J. Chem. Phys.* **1994**, *100*, 5792.

(42) Fan, P.-D.; Hirata, S. *J. Chem. Phys.* **2006**, *124*, 104108.

(43) Kállay, M.; Surján, P. R. *J. Chem. Phys.* **2001**, *115*, 2945.

(44) Kállay, M.; Szalay, P. G.; Gauss, J. *J. Chem. Phys.* **2002**, *117*, 980.

(45) Kowalski, K.; Hirata, S.; Włoch, M.; Piecuch, P.; Windus, T. L. *J. Chem. Phys.* **2005**, *123*, 074319.

(46) Slipchenko, V. L.; Krylov, I. A. *J. Chem. Phys.* **2005**, *123*, 084107.

(47) Gour, J. R.; Piecuch, P.; Włoch, M. *J. Chem. Phys.* **2006**, *123*, 134113.

(48) Gour, J. R.; Piecuch, P. *J. Chem. Phys.* **2006**, *125*, 234107.

(49) Gour, J. R.; Piecuch, P.; Włoch, M. *Int. J. Quantum Chem.* **2006**, *106*, 2854.

(50) Köhn, A.; Olsen, J. *J. Chem. Phys.* **2006**, *125*, 174110.

(51) Hirata, S. *J. Phys. Chem. A* **2003**, *107*, 9887.

(52) Hirata, S.; Fan, P.-D.; Auer, A. A.; Nooijen, M.; Piecuch, P. *J. Chem. Phys.* **2004**, *121*, 12197.

(53) Hirata, S. *J. Chem. Phys.* **2005**, *122*, 094105.

(54) Hirata, S. *Theor. Chem. Acc.* **2006**, *116*, 2.

(55) Hirata, S.; Bartlett, R. J. *Chem. Phys. Lett.* **2000**, *321*, 216.

(56) Hirata, S.; Nooijen, M.; Bartlett, R. J. *Chem. Phys. Lett.* **2000**, *326*, 255.

(57) Kállay, M.; Surján, P. R. *J. Chem. Phys.* **2000**, *113*, 1359.

(58) Olsen, J. *J. Chem. Phys.* **2000**, *113*, 7140.

(59) Salter, E. A.; Trucks, G. W.; Bartlett, R. J. *J. Chem. Phys.* **1989**, *90*, 1752.

(60) Sherrill, C. D.; Krylov, A. I.; Byrd, E. F. C.; Head-Gordon, M. *J. Chem. Phys.* **1998**, *109*, 4171.

(61) Krylov, A. I.; Sherrill, C. D.; Byrd, E. F. C.; Head-Gordon, M. *J. Chem. Phys.* **1998**, *109*, 10669.

(62) Krylov, A. I.; Sherrill, C. D.; Head-Gordon, M. *J. Chem. Phys.* **2000**, *113*, 6509.

(63) Koch, H.; Kobayashi, R. J. A.; de Merás, A. S.; Jørgensen, P. *J. Chem. Phys.* **1993**, *100*, 4393.

(64) Windus, T. L.; Pople, J. A. *Int. J. Quantum Chem. Suppl.* **1995**, *29*, 485.

(65) *NWChem, A Computational Chemistry Package for Parallel Computers, version 4.7*; Straatsma, T. P.; Aprà, E.; Windus, T. L.; Bylaska, E. J.; de Jong, W.; Hirata, S.; Valiev, M.; Hackler, M. T.; Pollack, L.; Harrison, R. J.; Dupuis, M.; Smith, D. M. A.; Nieplocha, J.; Tipparaju, V.; Krishnan, M.; Auer, A. A.; Brown, E.; Cisneros, G.; Fann, G. I.; Fruchtl, H.; Garza, J.; Hirao, K.; Kendall, R.; Nichols, J. A.; Tsemekhman, K.; Wolinski, K.; Anchell, J.; Bernholdt, D.; Borowski, P.; Clark, T.; Clerc, D.; Dachsel, H.; Deegan, M.; Dyall, K.; Elwood, D.; Glendening, E.; Gutowski, M.; Hess, A.; Jaffe, J.; Johnson, B.; Ju, J.; Kobayashi, R.; Kutteh, R.; Lin, Z.; Littlefield, R.; Long, X.; Meng, B.; Nakajima, T.; Niu, S.; Rosing, M.; Sandrone, G.; Stave, M.; Taylor, H.; Thomas, G.; van Lenthe, J.; Wong, A.; Zhang, Z. Pacific Northwest National Laboratory, Richland, WA, 2005.

(66) Christiansen, O.; Koch, H.; Jørgensen, P.; Olsen, J. *Chem. Phys. Lett.* **1996**, *256*, 185.

(67) Dunning, T. H., Jr. *J. Chem. Phys.* **1989**, *90*, 1007.

(68) Kendall, R. A.; Dunning, T. H., Jr.; Harrison, R. J. *J. Chem. Phys.* **1992**, *96*, 6796.

(69) Zachwieja, M. *J. Mol. Spectrosc.* **1995**, *170*, 285.

(70) Nelis, T.; Brown, J. M.; Evenson, K. M. *J. Chem. Phys.* **1990**, *92*, 4067.

(71) Kepa, R.; Para, A.; Rytel, M.; Zachwieja, M. *J. Mol. Spectrosc.* **1996**, *178*, 189.

(72) Huber, K. P.; Herzberg, G. *Molecular Spectra and Molecular Structure: Constants for Diatomic Molecules;* Van Nostrand Reinhold: New York, 1979.

(73) Phelps, D. H.; Dalby, F. W. *Phys. Rev. Lett.* **1966**, *16*, 3.

(74) Kasdan, A.; Herbst, E.; Lineberger, W. C. *Chem. Phys. Lett.* **1975**, *31*, 78.

(75) Steimle, T. C.; Nachman, D. F.; Fletcher, D. A.; Brown, J. M. *J. Mol. Spectrosc.* **1989**, *138*, 222.

(76) Takagi, K.; Oka, T. *J. Phys. Soc. Jpn.* **1963**, *18*, 1174.

(77) Fabricant, B.; Krieger, D.; Muenter, J. S. *J. Chem. Phys.* **1977**, *67*, 1576.

(78) Clouthier, D. J.; Ramsay, D. A. *Ann. Rev. Phys. Chem.* **1983**, *34*, 31.

(79) Freeman, D. E.; Klemperer, W. *J. Chem. Phys.* **1966**, *45*, 52.

(80) Yamaguchi, Y.; Sherrill, C. D.; Schaefer, H. F., III *J. Phys. Chem.* **1996**, *100*, 7911.

(81) Cramer, C. J.; Dulles, F. J.; Storer, J. W.; Worthington, S. E. *Chem. Phys. Lett.* **1994**, *218*, 387.

(82) Bauschlicher, C. W.; Langhoff, S. R.; Taylor, P. R. *J. Chem. Phys.* **1987**, *87*, 387.

(83) Sherrill, C. D.; Leininger, M. L.; Van Huis, T. J.; Schaefer, H. F., III *J. Chem. Phys.* **1998**, *108*, 1040.

(84) Van Huis, T. J.; Yamaguchi, Y.; Sherrill, C. D.; Schaefer, H. F., III *J. Phys. Chem. A* **1997**, *101*, 6955.

(85) Hoffman, B. C.; Yamaguchi, Y.; Schaefer, H. F., III *J. Phys. Chem. A* **1999**, *103*, 1886.

(86) Hirata, S.; Yanai, T.; Harrison, R. J.; Kamiya, M.; Fan, P.-D. *J. Chem. Phys.* **2007**, *126*, 024104.

CT600270C